Global Change Biology
celebrating 20 years

Global Change Biology (2015) **21**, 629–636, doi: 10.1111/gcb.12753

Viral attack exacerbates the susceptibility of a bloom-forming alga to ocean acidification

SHANWEN CHEN[1], KUNSHAN GAO[2] and JOHN BEARDALL[3]

[1]*Guangdong Provincial Key Laboratory of Marine Biology, Shantou University, Shantou 515063, China,* [2]*State Key Laboratory of Marine Environmental Science, Xiamen University, Xiamen 361005, China,* [3]*School of Biological Sciences, Monash University, Clayton Victoria 3800, Australia*

Abstract

Both ocean acidification and viral infection bring about changes in marine phytoplankton physiological activities and community composition. However, little information is available on how the relationship between phytoplankton and viruses may be affected by ocean acidification and what impacts this might have on photosynthesis-driven marine biological CO_2 pump. Here, we show that when the harmful bloom alga *Phaeocystis globosa* is infected with viruses under future ocean conditions, its photosynthetic performance further decreased and cells became more susceptible to stressful light levels, showing enhanced photoinhibition and reduced carbon fixation, up-regulation of mitochondrial respiration and decreased virus burst size. Our results indicate that ocean acidification exacerbates the impacts of viral attack on *P. globosa*, which implies that, while ocean acidification directly influences marine primary producers, it may also affect them indirectly by altering their relationship with viruses. Therefore, viruses as a biotic stressor need to be invoked when considering the overall impacts of climate change on marine productivity and carbon sequestration.

Keywords: CO_2, ocean acidification, *Phaeocystis globosa*, photosynthesis, virus

Received 15 June 2014; revised version received 6 September 2014 and accepted 8 September 2014

Introduction

The oceans are experiencing a range of changes, including a marked acidification as anthropogenic CO_2 dissolves in surface waters. In parallel, phytoplankton cells are also exposed to natural seawater acidification associated with eutrophication (Sunda & Cai, 2012) and upwelling processes (Capone & Hutchins, 2013) as well as biological activities (Flynn *et al.*, 2012). Such compounded changes in pH and carbonate chemistry, along with other environmental forcings, are predicted to bring about changes in productivity and community composition of marine phytoplankton (Beardall *et al.*, 2009a; Kroeker *et al.*, 2010; Gao *et al.*, 2012a,b) as well as consequences for higher trophic levels (Kroeker *et al.*, 2013; Rossoll *et al.*, 2013; Constable *et al.*, 2014).

Viruses are an important constituent of oceanic ecosystems and can impair the metabolic machinery of infected photosynthetic organisms (Juneau *et al.*, 2003; Brussaard *et al.*, 2007; Weitz & Wilhelm, 2012), which can produce dramatic crashes in populations and changes in primary productivity (Bratbak & Jacobsen, 1998; Suttle, 2007; Danovaro *et al.*, 2011); on the other hand, viruses may potentially stimulate primary production by enhancing nutrient cycling (Weinbauer *et al.*, 2011; Shelford *et al.*, 2012; Staniewski & Short, 2014). Any influence of global climate change on virus-algae interactions is thus likely to modulate the significant ecological consequences of those interactions (Danovaro *et al.*, 2011). Although algal viruses are becoming better understood, little information is available on how this relationship may be affected by climate change forcings and what impacts this might have on the marine biological CO_2 pump, which drives the absorption of atmospheric CO_2 into the oceans. Ocean acidification, as one of the most influential global changes to ocean ecosystems, has been shown to reduce the abundance of *Emiliania huxleyi* virus (Larsen *et al.*, 2008), or increase its burst size, and delay lysisof its hosts (Carreira *et al.*, 2012). Decreasing pH also had profound effects on the infection capacity of a cyanobacterial virus and its infection cycle in an oceanic cyanobacterium, *Synechococcus* WH7803 (Traving *et al.*, 2013). However, none of these studies have linked changes in infection under ocean acidification conditions to the physiological performance of the algae/cyanobacteria.

Phaeocystis is an important algal genus in both coastal and offshore waters, particularly in colder temperate regions, where the species (mainly *P. pouchetii* and *P. globosa*) can form extensive blooms, locking up vast amounts of carbon and nutrients in algal biomass (Schoemann *et al.*, 2005; Brussaard *et al.*, 2007; Danov-

Correspondence: Kunshan Gao, tel. 86-592-2187982, fax 86-592-2187963, e-mail: ksgao@xmu.edu.cn

© 2014 John Wiley & Sons Ltd

aro *et al.*, 2011). Virus infection can trigger the collapse of such blooms and consequently exert tremendous influence on carbon dynamics and nutrient recycling in marine ecosystems (Brussaard *et al.*, 2005; Danovaro *et al.*, 2011). We have recently shown that *Phaeocystis globosa* responds to ocean acidification by acclimation in its photosynthetic machinery (Chen & Gao, 2011, Chen *et al.*, 2014). Here, we extend this work to show results of investigations into the influence of ocean acidification on the interaction between *P. globosa* and its associated virus (PgV). We studied the coupled effects of viral infection and seawater acidification on the photosynthetic performance and mitochondrial respiration in *P. globosa* cells. We also measured impacts of seawater acidification on viral burst size, to understand mechanisms involved in the virus-alga relationship.

Materials and methods

Organisms and growth conditions

Phaeocystis globosa Scherffel (ST-97), used in this study, was isolated from a bloom in the Southern China Sea in 1997 and has subsequently been maintained at Xiamen University, China. Only the flagellated form, which is the dominant morphological form of *P. globosa* during the species' life cycle (Rousseau *et al.*, 2007), was used here. All cultures of the alga were grown axenically at 15 °C in modified (silicate was not enriched) f/2 medium under 200 μmol photons m^{-2} s^{-1} (PAR) and a 12 : 12 light dark cycle and with aeration by ambient CO_2 (~390 μatm at the time the experiments were carried out) or 1000 μatm CO_2 in air, as described previously (Chen & Gao, 2011). The culture was rendered axenic by treatment with a mixture of the antibiotics carbenicillin and cefotaxime, and growth on yeast extract for 9 days, according to Brussaard *et al.* (1999), and was thereafter maintained in continuous culture according to Chen & Gao (2011).

The elevated pCO_2 of 1000 μatm, representing the predicted (IPCC A1F1 scenario) pCO_2 in the atmosphere by 2100 (LaRoche *et al.*, 2010), was achieved using an illuminated CO_2 chamber (Conviron EF7; Controlled Environments Limited, Winnipeg, Canada), in which the CO_2 concentration in air was automatically achieved by mixing pure CO_2 and ambient air. The CO_2-enriched air within the chamber led to a lowered pH_{nbs} of 7.7 (LpH culture), increased bicarbonate ion concentration by 12.4% and decreased carbonate ions by 51.4%, compared to that of the ambient CO_2 level, which was achieved by aerating cultures with outdoor air of 390 μatm CO_2 [pH_{nbs} 8.07 (HpH culture)]. The pH_{nbs} and concentrations of bicarbonate and carbonate ions in cultures equilibrated with the ambient CO_2 level were 8.07, 1793.9 μM and 208.7 μM, respectively. These parameters of the seawater carbonate system were determined according to Chen & Gao (2011) and are reported in Table S1.

The flagellated cells (3–8 μm) were grown for nine generations at the corresponding CO_2 levels before experiments were carried out. In the short-term incubations to measure photosynthetic characteristics and respiration, after harvesting cells by centrifugation and resuspending them in fresh medium, we adjusted the pH to target values (7.70/1000 μatm CO_2) by injecting CO_2-saturated seawater (Gattuso & Lavigne, 2010). All experiments were run with three independent cultures, the noninfected controls of which were treated by addition of an equal volume of autoclaved viral lysate.

Isolation and cloning of PgV

Viruses of *Phaeocystis globosa* (PgVs) were isolated, in November 2007, from the coastal waters of Shantou (23.3°N, 116.6°E), when the algal bloom occurred. Seawater (10 l) was sampled at the end point of the algal bloom and filtered through 0.2 μm pore-size cellulose acetate filters (Schleicher and Schuell GmbH, Dassel, Germany). The filtrate was then concentrated, by an ultrafiltration disc (PM30, Amicon, High Wycombe, Bucks, UK), to 100 ml, according to established protocols (Suttle *et al.*, 1991; Brussaard *et al.*, 2004; Nagasaki & Bratbak, 2010). The concentrated virus-size fraction was used for inocula, and the clonal isolate of PgV was obtained by a modified serial infection procedure according to Brussaard (2004) (see supporting information for full details) and confirmed by staining with SYBR Green Iand flow cytometer measurements (FACSaria, BD, San Jose, CA, USA) (Brussaard, 2004; Baudoux *et al.*, 2006). The flow cytometry signature (Figure S1) indicated that in addition to PgVs, there was some noise in the 0.2 μm pore-size filtrate from the clonal isolate of PgV-infected *P. globosa* cultures, which could be DNA segments and organelles from the lysis of host cells.

Algal and viral counts

The cells of *P. globosa* were enumerated directly after sampling using flow cytometry (FACSaria, Becton Dickinson) and algal chlorophyll fluorescence (Marie *et al.*, 1999).

Virus enumeration was also carried out by flow cytometry after staining according to Marie *et al.* (1999) and Brussaard (2004). The brief procedures were as follows: (i) The filtrate, passed through 0.2 μm pore-size cellulose acetate filters, was fixed with glutaraldehyde (0.5% final concentration) for 20 min, and then stored at −80 °C after snap freezing in liquid nitrogen; (ii) The fixed frozen samples were thawed at room temperature, diluted in TE buffer (Tris 10 mM, EDTA 1 mM, pH 7.5), and then incubated for 15 min in the dark at 80 °C after the green fluorescent nucleic acid specific dye SYBR Green I (final concentration 0.5 * 10^{-4} commercial stock) had been added; (ii) The stained virus particles were enumerated using flow cytometry at event rates of 100–1000 events s^{-1} (FACSaria, Becton Dickinson, USA).

Determinations of photosynthetic activity and dark respiration

The results of preliminary experiments showed that the length of time from inoculation by PgV to significant decrease in photochemical efficiency was less than 12 h, so the determinations

of oxygen exchange were carried out 12 h after the PgVs were added.

Relative electron transport rates (rETRs) were determined using a pulse amplitude modulated fluorometer (PAM, WATER-PAM, Walz, Germany). Rapid light curves (RLCs) and the photosynthetic parameters α (photosynthetic light harvesting efficiency), β (a photoinhibitory term), $rETR_{max}$ (maximal rETR) and I_k (light saturation point) were obtained by fitting the rETR data to a double exponential function (Platt *et al.*, 1980): $rETR = rETR_m * [1 - e^{-(\alpha * I/rETRm)}] * e^{-\beta * I/rETRm}$, where I represents the irradiance under which rETR was measured. The effective quantum yield ($\Delta F/F_m' = (F_m' - F_t)/F_m'$) was determined on the basis of measurements of the maximal fluorescence (F_m') and the steady-state fluorescence (F_t) of the light-adapted cells (Genty *et al.*, 1989), with an actinic light level of 200 μmol photons m^{-2} $s^{-1}$and a saturating pulse intensity of 4000 μmol photons m^{-2} s^{-1} (0.8 s).

Photosynthetic oxygen evolution and dark respiration rates were measured with a Clark-type O_2 electrode (YSI 5300; Yellow Springs, Dayton, OH, USA). Cells were grown at the high-pH/low CO_2 (HpH) or low-pH/high CO_2 (LpH) levels for nine generations in a modified continuous culture system (Chen & Gao, 2011) before measurements were taken. In the case of viral infected cells, cultures were inoculated with PgVs (at PgV: host = 20: 1 by number), and then incubated under the relevant growth conditions for 12 h before measurements commenced.

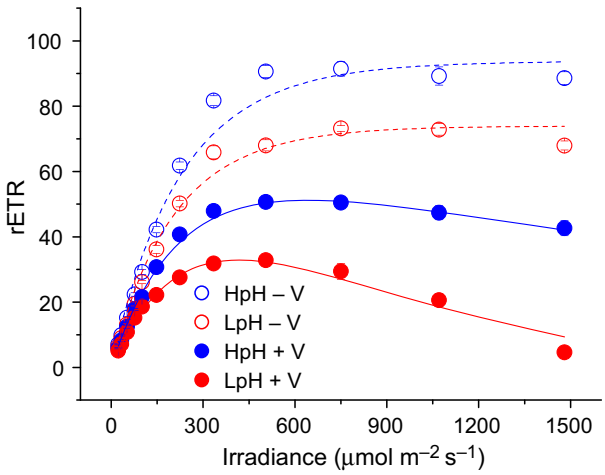

Fig. 1 Relative electron transport rate (rETR) as a function of light in *Phaeocystis globosa* cells grown at ambient CO_2 of 390 (pH_{nbs} of 8.07, HpH) or 1000 μatm CO_2 (pH_{nbs} of 7.70, LpH) levels being uninfected (−V) or infected (+V) by its virus. The cells had been grown in continuous cultures under the two CO_2 levels for nine generations before being infected with PgV, and the measurements were taken 12 h later. The data represent means ± SD (n = 3, triplicate incubations).

Burst size estimation

To estimate the burst size, the latent period of PgV was assessed in preliminary experiments to be less than 12 h, and the concentration of *P. globosa* cells and PgVs, after PgVs had been added to the algal culture, were determined at the same time every day.

Burst size, the number of viruses produced per lysed cell (or viruses released per lytic cycle), was estimated according to Weinbauer *et al.* (2010) as follows: Burst size = (maximum − minimum viral abundance)/number of lysed cells. Our data indicated that there were host cells remaining when the number of PgVs was up to a maximum during the release of PgVs, so the number of lysed cells in this study was calculated from the maximum cell number minus the remaining host cell number during the release of PgVs.

The estimates of burst size were carried out under the ambient and the high CO_2 levels mentioned above. The cultures were acclimated to the relevant growth conditions for about nine generations before the viruses were added. The viruses and their hosts were enumerated with flow cytometry, and *in vivo* chlorophyll fluorescence was monitored using the Water-PAM. The cell abundance and specific growth rate of the alga were maintained in the continuous cultures at between 5.6 and 5.9 × 10^5 cells ml^{-1}, and between 1.1 and 1.3 d^{-1}, respectively, except in the relevant cultures after the viruses were added.

Statistical analysis

Data was analyzed in GraphPad Prism 6.0, using a one-way or two-way ANOVA. A P value of <0.05 was used to indicate statistical significance. In the case of the rETR vs irradiance relationships (Rapid Light Curves, RLCs), the whole rETR vs irradiance data set was subjected to Principal Component

Table 1 The light harvesting efficiency (α), maximum relative electron transport rate ($rETR_m$), light saturation point (I_k) and photoinhibitory characteristic (β), derived from the rapid light curves (Fig. 1), for *Phaeocystis globosa* cells uninfected (−V) or infected (+V) by its virus under ambient CO_2 (HpH) or high CO_2 (LpH). Superscripts with different letters represent significant difference (P < 0.05) among the treatments. The data represent means ± SD (n = 3)

	α	rETRm (μmol photons m^{-2} s^{-1})	I_k (μmol photons m^{-2} s^{-1})	β
HpH − V	0.36 ± 0.03^a	120.1 ± 19.5^e	333.6 ± 13.1^m	0.001 ± 0.001^r
LpH − V	0.33 ± 0.01^b	96.3 ± 11.5^f	291.8 ± 8.3^q	0.002 ± 0.001^r
HpH + V	0.28 ± 0.02^c	59.6 ± 7.3^g	212.9 ± 8.9^n	0.013 ± 0.001^s
LpH + V	0.22 ± 0.01^d	33.7 ± 5.9^h	153.2 ± 7.3^p	0.025 ± 0.001^t

Analysis (PCA) using The Unscrambler X v 10.2 (Camo Inc., Oslo, Norway).

Results

Photosynthetic characteristics and respiration

Under ambient CO_2 levels, the quantum yield and cell concentration of *Phaeocystis globosa* after infection with PgVs decreased with the increased abundance of the virus (Figure S2). Viral infection caused a drop in electron transport rates (rETR), especially at higher photon fluxes (Fig. 1). Growth at high CO_2 (low pH) also caused a drop in rETR, which was exacerbated when cells were infected with the virus. Viral infection also caused a more marked photoinhibition (β) in both high- and ambient-CO_2 grown cultures (Fig. 1; Table 1), but this stimulation of photoinhibition was especially marked under high-CO_2 (LpH + V treatment). This was supported by the results of the two-way ANOVA, which indicated a very significant interaction between CO_2 level and virus infection for the photoinhibition term (Table 2). Principal components analysis (PCA) of the RLC data from Fig. 1 showed a

Table 2 Results of two-way ANOVA for photosynthetic parameters and dark respiration in +/− virus-treated and high- or ambient-CO_2 treatments

Response variable	Source of variation	SS	DF	MS	F	*P* value
$rETR_m$	CO_2 level	1853	1	1853	15.62	0.0042
	Virus	11365	1	11365	95.81	<0.0001
	Interaction	3.308	1	3.308	0.02788	0.8715
Alpha (α)	CO_2 level	0.00559	1	0.00559	18.45	0.0026
	Virus	0.02736	1	0.02736	90.32	<0.0001
	Interaction	0.00063	1	0.00063	2.082	0.1870
Beta (β)	CO_2 level	0.0001141	1	0.0001141	152.1	<0.0001
	Virus	0.0008841	1	0.0008841	1179	<0.0001
	Interaction	0.001141	1	0.0001141	152.1	<0.0001
I_k	CO_2 level	7727	1	7727	104.9	<0.0001
	Virus	50427	1	50427	684.5	<0.0001
	Interaction	240.3	1	240.3	3.262	0.1085
Net PS (Pn)	CO_2 level	0.001102	1	0.001102	1.190	0.3072
	Virus	0.01184	1	0.01184	12.78	0.0072
	Interaction	6.750e-006	1	6.750e-006	0.007286	0.9341
Dark respiration	CO_2 level	0.0003413	1	0.0003413	20.58	0.0019
	Virus	0.001633	1	0.001633	98.49	<0.0001
	Interaction	1.333e-006	1	1.333e-006	0.08040	0.7840

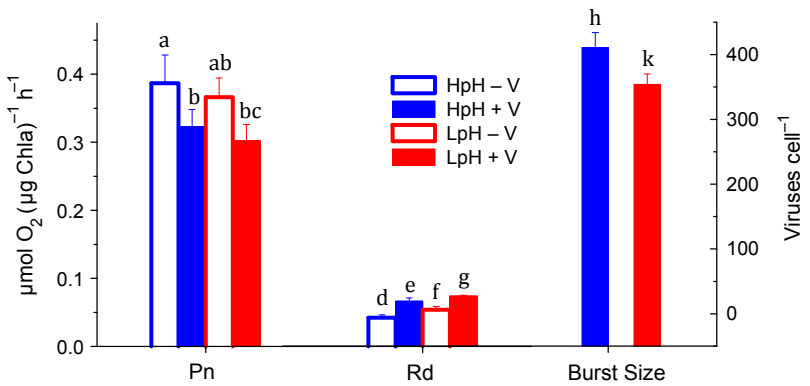

Fig. 2 Effects of ocean acidification on the interaction of *P. globosa* with its virus. HpH represents pH_{nbs}8.07; LpH, pH_{nbs}7.70; V, virus; P_n, net photosynthesis; R_d, dark respiration. Different superscript letters represent significant differences ($P < 0.05$) among the treatments. The data represent means ± SD ($n = 3$).

strong clustering along PC1, which explains 99.4% of the variance in the data set (Figure S3, upper panel). The loadings plot (Figure S3, lower panel) demonstrates that rETR is higher for virus-free cultures at all irradiances, but this becomes more evident as irradiance increases, an observation consistent with the effects on photoinhibition described above.

Thus both the CO_2 levels and the virus had effects on the photosynthetic performance, with the greatest influence being the presence or absence of the virus. Lowered pH (elevated CO_2) alone caused a decrease of 8.3% in light harvesting efficiency (α), 19.8% (from 120.1 to 96.3) in light saturated electron transport rates ($rETR_m$), and 12.5% in light saturation point (I_k) in *P. globosa* cells, which dropped by a further 33.3%, 65.4% and 47.5% respectively with infection of PgVs; in addition, the viral infection caused marked photoinhibition (β) in both high- and low-pH grown cultures (Tables 1 and 2). Within each of these virus-treatment groups, the ambient CO_2 treatment always produced the highest ETRs. Both CO_2 treatment and virus infection caused large, statistically significant, differences in $rETR_m$, α, I_k and β (Tables 1 and 2). While high-CO_2 and virus-infected cells had the lowest values for $rETR_{max}$, I_k and α, there was no statistically significant interaction between virus infection and CO_2 level (Table 2) for any parameter other than photoinhibition.

Lowered pH alone did not cause a significant decrease in rates of photosynthetic O_2 evolution. However, viral infection reduced the rates by 16.6% in the high-pH and by 16.7% in the low-pH grown *P. globosa* cells (Fig. 2, Table 2). However, the rates were significantly lower by 22.8% in the infected high-CO_2 (LpH + V) grown cells compared to those grown under the ambient-CO_2 (HpH), with the acidification effect responsible for 5.4% of this decrease. In contrast, both Low-pH treatment and viral infection significantly increased the alga's mitochondrial respiration by 28.6% and 56.7%, respectively (Fig. 2; Table 2). In the ambient CO_2 grown cells, the stimulation of respiration following infection was 57.4%, but in the high CO_2 grown cells, the stimulation after infection was 36.8%. As with measurements of electron transport, there were statistically significant effects of virus infection and of CO_2 level (Table 2), but no statistically significant interaction between virus infection and CO_2 levels for either respiration or photosynthetic O_2 evolution (Table 2).

Burst size

Preliminary experiments showed that the latent period of PgV infection was 11.7 h and 11.9 h in the high-pH (low-CO_2) and the low-pH (high-CO_2) cultures respectively, this difference being statistically insignificant (data not shown).

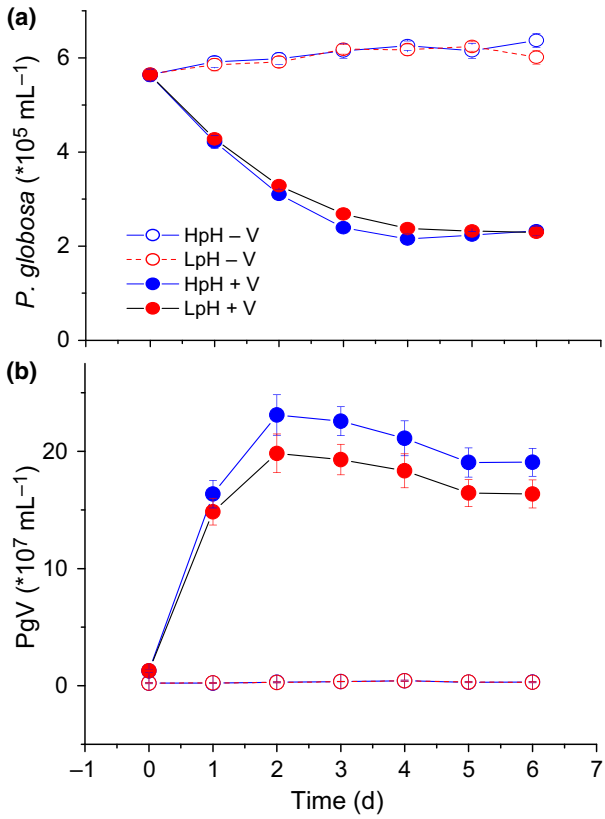

Fig. 3 Changes in cell (a) and virus (b) concentration of *P. globosa* during the burst size determination under different CO_2 (pH) treatments. HpH (=ambient CO_2) represents pH_{nbs}8.07; LpH (=high CO_2), pH_{nbs}7.70; V, virus. The data represent mean ± SD (n = 3, triplicate cultures).

The burst size of PgV was affected by the CO_2 level/pH (Figs 2 and 3). In the ambient-CO_2- and the high-CO_2-grown cells, burst size was 354 and 305 viruses per cell, respectively, thus decreasing by 13.9% for the high-CO_2-grown cells (F = 15.074, P = 0.0178). It is interesting in this context to note that the lower numbers of PgV released under high CO_2 (LpH; Fig. 3b) align with the slower decline in *Phaeocystis* cell numbers following infection under these conditions, with rate constants for the exponential decay in cell numbers of 0.618 ± 0.0026 and 0.546 ± 0.0028 d^{-1} (P = 0.0014) in infected ambient- and high-CO_2-grown cells, respectively (Fig. 3).

Discussion

Ocean acidification is known to have profound effects on the physiological performance of many algae (Beardall *et al.*, 2009b; Riebesell & Tortell, 2011; Gao *et al.*, 2012a,b) and *P. globosa* is no exception, showing

dynamic changes in its photosynthetic performance under elevated CO_2 (Chen & Gao, 2011, Chen *et al.*, 2014). Virus infection of *P. globosa* under ambient CO_2 caused a decrease in quantum yield and cell concentration, as expected from previous reports, with the burst size of 354 viruses per cell (Brussaard *et al.*, 2007). However, the determinations of photosynthetic characteristics (Figs 1 and 2; Table 1) showed that viral infection caused more negative effects on *P. globosa* under the high-CO_2-induced acidification. This was especially true for photoinhibition, which doubled in virus-infected cells under high CO_2, but was essentially absent in noninfected cells, independent of CO_2. This observation is especially important for a surface-bloom-forming genus such as *Phaeocystis*. The interplay of rising CO_2 and virus infection on a bloom-forming marine alga, reported here, implies that the virus-host relationship will be influenced by ocean acidification, resulting in decreased photosynthetic energy transfer and enhanced respiratory carbon loss.

In the marine cyanobacterium *Synechococcus* WH 7803 infected with the virus, lowered pH led to shorter latent period, smaller burst size and longer eclipse phase (Traving *et al.*, 2013). While decreased photosynthetic carbon fixation has been shown in natural phytoplankton assemblages after infection with a virus fraction (Suttle, 1992) and changes in quantum yield of photosystem II of *Phaeocystis pouchetii* following viral infection have been previously demonstrated (Brussaard *et al.*, 2007), the present study provided evidence that future ocean conditions or dynamic pH changes in coastal waters, decrease the photosynthetic performance of *P. globosa* further, increase its mitochondrial respiration and decrease the virus burst size, as compared to virus-infected cells under the present-day CO_2 level. Importantly, although there was no interaction between acidification and virus infection for most photosynthetic parameters, there were strong interactive effects on photoinhibition, implying that ocean acidification and viral infection combined would exacerbate the susceptibility of cells to the high light intensities in surface waters.

Viral infection significantly increased the alga's respiratory rates in the cells exposed to both the ambient and the high CO_2. The infection caused a lower stimulation in the high CO_2 grown cells than that in the ambient CO_2 grown cells. In a previous study (Eissler *et al.*, 2003), virus infection of the picophytoplankter *Mantoniella* sp. caused a marked decrease in respiration, whereas in *Micromonas pusilla*, infection led to an increase in respiration, though it should be noted that in this work respiration was uncorrected for algal biomass or cell numbers. In another report (Eissler & Quiñones, 2003), respiratory rates of *Cyclotella* marginally increased or decreased depending on the size of the viral inoculum. On the assumption that the PgV relies on host metabolism to produce new viral units, this may be reflected in the observed reduced photosynthetic energy transfer and stimulated mitochondrial respiration following infection.

The lower stimulation of respiration following infection of cells grown under the high CO_2 (LpH) conditions may thus be associated with the significantly lower subsequent burst size in high CO_2 grown cells (Figs 2 and 3). Diminished photosynthetic energy supply could have led to decreased energy availability for the virus to propagate, consequently resulting in a smaller burst size. This in turn may be associated with the generally more stressed metabolic state of cells growing under the ambient pH conditions, which was supported by the fact that the decline in *Phaeocystis* cell numbers following infection was slower in high CO_2 (LpH) cells than that in infected ambient-CO_2 grown cells (Fig. 3), a feature also consistent with lowered stimulation of respiration by virus infection under the more acidic conditions.

The pH drop associated with ocean acidification is reported to cause alterations in viral populations, with species-specific viral responses to pH change (Larsen *et al.*, 2008; Danovaro *et al.*, 2011), and changes in virus-host interactions (Carreira *et al.*, 2012; Traving *et al.*, 2013), which may act to alter community composition and structure of phytoplankton populations. Most of the studies on pH effects reported to date have concerned the infection cycle of viruses in relation to ocean acidification, rather than direct effects on the virus, though Traving *et al.* (2013) reported no effect of pH on decay of cyanophage S-PM2 in seawater, with solar irradiance being the main determinant of viral particle decay (Suttle & Chen, 1992). The 0.4-unit drop in pH used here caused a decrease inburst size (Fig. 2), and interacted with PgVs on *P. globosa* to cause an increase in susceptibility to high light (Fig. 1), a decrease in photosynthesis, and a stimulation of mitochondrial respiration (Fig. 2). This suggests that marine carbon cycle, for which phytoplankters like *P. globosa* are key players, would be affected by increased light exposure due to enhanced stratification associated with global warming and by ocean acidification in the presence of virus. If the interaction of pH drop and virus observed in this work occurs in other primary producers, formation of particulate organic carbon (POC) will decrease with progressive ocean acidification. Viral-induced lysis releases large amounts of dissolved organic carbon (DOC) (Miki *et al.*, 2008; Danovaro *et al.*, 2011), which is then open to break down and nutrient recycling through the microbial food web. However, the observation that burst size is diminished under ocean

acidification suggests that viral infection may not propagate as rapidly in a future ocean, altering the balance between DOC processing by the microbial food web and sinking of POC to the deep ocean where it can be sequestered. In this respect, it is important to note that colonial forms of *Phaeocystis pouchetii* (which because of their larger size might be expected to sink more rapidly and therefore play a bigger role in C sequestration than the unicellular form) appear to not be susceptible to viral infection (Jacobsen *et al*., 2007). Coloniality may influence viral infections in a number of ways, though whether the reduced infection is due to the presence of a pellicle around the colonies (Hamm *et al*., 1999), chemically induced apoptosis reducing burst size or reduced encounter rates between virus and cells is uncertain (Beardall *et al*., 2009a,b).

This influence of virus on nutrient cycling is also reflected in consequences for sulfur biogeochemistry. *Phaeocystis* and coccolithophores produce large amounts of dimethylsulfoniopropionate (DMSP) thought to be important as an osmoticum and scavenger of reactive oxygen species (Larsen, 2013). Viral lysis of *Phaeocystis* cells has been suggested to be an important mechanism for the release of DMSP and related S-containing compounds (Malin *et al*., 1998). Given that elevated CO_2 is reported to cause a reduction in cellular production rates of DMSP (Larsen, 2013), decreased lysis under ocean acidification is likely to further reduce S release and recycling.

In conclusion, the present data indicated that (i) infection with PgV has a significant impact on photosynthetic electron transport; (ii) this effect is greater under ocean acidification; (iii) viral infection significantly increased the alga's respiratory rates in the cells exposed to both ambient and high CO_2, and the stimulation was lower in the high-CO_2-grown cells than that in the ambient-CO_2-grown cells; and (iv) the 0.4 unit change in pH caused a decrease in burst size. These observations suggest that, while ocean acidification directly brings about changes in productivity and community composition of marine phytoplankton, it may also indirectly affect them by altering the relationship between the producer and its virus, which indicates yet another interaction that needs to be invoked when considering the overall impacts of climate change on marine productivity and carbon cycling, even the release of DMSP and related S-containing compounds.

Acknowledgements

This study was supported by Joint project of NSFC and Shandong province (Grant No. U1406403), National Natural Science Foundation (41120164007, 41430967), Strategic Priority Research Program of CAS (Grant No. XDA11020302),Program for Changjiang Scholars and Innovative Research Team (IRT_13R51), SOA (GASI-03-01-02-04) and China-Japan collaboration project from MOST (S2012GR0290). JB's work on climate change effects on algae has been funded by the Australian Research Council and his visit to Xiamen was supported by '111' project from Ministry of Education. The authors are grateful to Dr Philip Heraud at Monash University for advice on multivariate approaches to analyzing our data.

References

Baudoux AC, Noordeloos AA, Veldhuis MJ, Brussaard CP (2006) Virally induced mortality of *Phaeocystis globosa* during two spring blooms in temperate coastal waters. *Aquatic Microbial Ecology*, **44**, 207–217.

Beardall J, Stojkovic S, Larsen S (2009a) Living in a high CO_2 world: impacts of global climate change on marine phytoplankton. *Plant Ecology and Diversity*, **2**, 191–205.

Beardall J, Allen A, Bragg J *et al*. (2009b) Allometry and stoichiometry of unicellular, colonial and multicellular phytoplankton. *New Phytologist*, **181**, 295–309.

Bratbak G, Jacobsen AM (1998) Viral lysis of *Phaeocystis pouchetii* and bacterial secondary production. *Aquatic Microbial Ecology*, **11**, 11–16.

Brussaard CP, Thyrhaug R, Marie D, Bratbak G (1999) Flow cytometric analyses of viral infection in two marine phytoplankton species, *Micromonas pusilla* (Prasinophyceae) and *Phaeocystis pouchetii* (Prymnesiophyceae). *Journal of Phycology*, **35**, 941–948.

Brussaard CPD (2004) Optimization of procedures for counting viruses by flow cytometry. *Applied and Environmental Microbiology*, **70**, 1506–1513.

Brussaard CPD, Short SM, Frederickson CM, Suttle CA (2004) Isolation and phylogenetic analysis of novel viruses infecting the phytoplankton *Phaeocystis globosa* (Prymnesiophyceae). *Applied and Environmental Microbiology*, **70**, 3700–3705.

Brussaard CPD, Kuipers B, Veldhuis MJW (2005) A mesocosm study of *Phaeocystis globosa* population dynamics. I. Regulatory role of viruses in bloom control. *Harmful Algae*, **4**, 859–874.

Brussaard CPD, Bratbak G, Baudoux AC, Ruardij P (2007) *Phaeocystis* and its interaction with viruses. *Biogeochemistry*, **83**, 201–215.

Constable AJ, Melbourne-Thomas J, Corney SP *et al*. (2014) Climate change and Southern Ocean ecosystems I: how changes in physical habitats directly affect marine biota. *Global Change Biology*, **20**, 3004–3025.

Capone DG, Hutchins DA (2013) Microbial biogeochemistry of coastal upwelling regimes in a changing ocean. *Nature Geoscience*, **6**, 711–717.

Carreira C, Heldal M, Bratbak G (2012). Effect of increased pCO_2 on phytoplankton–virus interactions. *Biogeochemistry*, **113**, 391–397.

Chen SW, Gao KS (2011) Solar ultraviolet radiation and CO_2-induced ocean acidification interacts to influence the photosynthetic performance of the red tide alga *Phaeocystis globosa* (Prymnesiophyceae). *Hydrobiologia*, **675**, 105–117.

Chen SW, Beardall J, Gao KS (2014) A red tide alga grown under ocean acidification upregulates its tolerance to lower pH by increasing its photophysiological functions. *Biogeosciences*, **11**, 4829–4838.

Danovaro R, Corinaldesi C, Dell'Anno A, Fuhrman JA, Middelburg JJ, Noble RT, Suttle CA (2011) Marine viruses and global climate change. *FEMS Microbiology Reviews*, **35**, 993–1034.

Eissler Y, Sahlsten E, Quiñones RA (2003) Effects of virus infection on respiration rates of marine phytoplankton and microplankton communities. *Marine Ecology Progress Series*, **262**, 71–80.

Eissler Y, Quiñones RA (2003) The effect of viral concentrate addition on the respiration rate of *Chaetoceros gracilis* cultures and microplankton from a shallow bay (Coliumo, Chile). *Journal of Plankton Research*, **25**, 927–938.

Flynn KJ, Blackford JC, Baird ME *et al*. (2012) Changes in pH at the exterior surface of plankton with ocean acidification. *Nature Climate Change*, **2**, 510–513.

Gao KS, Helbling EW, Häder DP, Hutchins DA (2012a) Responses of marine primary producers to interactions between ocean acidification, solar radiation, and warming. *Marine Ecology Progress Series*, **470**, 167–189.

Gao KS, Xu J, Gao G *et al*. (2012b) Rising CO_2 and increased light exposure synergistically reduce marine primary productivity. *Nature Climate Change*, **2**, 519–523.

Gattuso J, Lavigne H (2010) Perturbation experiments to investigate the impact of ocean acidification: approaches and software tools. *Biogeosciences*, **6**, 4413–4439.

Genty B, Briantais JM, Baker NR (1989) The relationship between the quantum yield of photosynthetic electron transport and quenching of chlorophyll fluorescence. *Biochimica et Biophysica Acta*, **990**, 87–92.

Hamm CE, Simson DA, Merkel R, Smetacek V (1999) Colonies of *Phaeocystis globosa* are protected by a thin but tough skin. *Marine Ecology Progress Series*, **187**, 101–111.

Jacobsen A, Larsen A, Martinez-Martinez J, Verity PG, Frischer ME (2007) Susceptibility of colonial cells of *Phaeocystis pouchetti* (Haptophyta) to viral infection. *Aquatic Microbial Ecology*, **48**, 105–112.

Juneau P, Lawrence JE, Suttle CA, Harrison PJ (2003) Effects of viral infection on photosynthetic processes in the bloom-forming alga *Heterosigma akashiwo*. *Aquatic Microbial Ecology*, **31**, 9–17.

Kroeker KJ, Kordas RL, Crim RN, Singh GG (2010) Meta-analysis reveals negative yet variable effects of ocean acidification on marine organisms. *Ecology Letters*, **13**, 1419–1434.

Kroeker KJ, Kordas RL, Crim R, Hendriks IE, Ramajo L, Singh GS, Gattuso JP (2013) Impacts of ocean acidification on marine organisms: quantifying sensitivities and interaction with warming. *Global Change Biology*, **19**, 1884–1896.

LaRoche J, Rost B, Engel A (2010). Bioassays, batch culture and chemistat experimentation. In: *Guide to Best Practices in Ocean Acidification Research and Data Reporting* (eds Riebesell U, Fabry VJ, Hansson L, Gattuso J), pp. 81–94. Publications Office of the European Union, Luxembourg.

Larsen JB, Larsen A, Thyrhaug R, Bratbak G, Sandaa RA (2008) Response of marine viral populations to a nutrient induced phytoplankton bloom at different pCO_2 levels. *Biogeosciences*, **5**, 523–533.

Larsen S (2013). Dimethylsulphoniopropionate (DMSP) production in *Gephryocapsa oceanica* in response to environmental forcing. PhD Thesis, pp.182. Monash University, Australia.

Malin G, Wilson WH, Bratbak G, Liss PS, Mann NH (1998) Elevated production of dimethylsulfide resulting from viral infection of cultures of *Phaeocystis pouchetii*. *Limnology and Oceanography*, **43**, 1389–1393.

Marie D, Brussaard CP, Thyrhaug R, Bratbak G, Vaulot D (1999) Enumeration of marine viruses in culture and natural samples by flow cytometry. *Applied and Environmental Microbiology*, **65**, 45–52.

Miki T, Nakazawa T, Yokokawa T, Nagata T (2008) Functional consequences of viral impacts on bacterial communities: a food-web model analysis. *Freshwater Biology*, **53**, 1142–1153.

Nagasaki K, Bratbak G (2010). Isolation of viruses infecting photosynthetic and nonphotosynthetic protists. In: *Manual of Aquatic Viral Ecology* (eds Wilhelm SW, Weinbauer MG, Suttle CA), pp. 92–101. ASLO, Waco.

Platt T, Gallegos CL, Harrison WG (1980) Photoinhibition of photosynthesis in natural assemblages of marine phytoplankton. *Journal of Marine Research*, **38**, 687–701.

Riebesell U, Tortell PD (2011). Effects of ocean acidification on pelagic organisms and ecosystems. In: *Ocean Acidification* (eds Gattuso JP, Hansson L), pp. 291–311. Oxford University Press, New York.

Rossoll D, Sommer U, Winder M (2013) Community interactions dampen acidification effects in a coastal plankton system. *Marine Ecology Progress Series*, **486**, 37–46.

Rousseau V, Chrétiennot-Dinet MJ, Jacobsen A, Verity P, Whipple S (2007) The life cycle of *Phaeocystis*: state of knowledge and presumptive role in ecology. *Biogeochemistry*, **83**, 29–47.

Schoemann V, Becquevort S, Stefels J, Rousseau V, Lancelot C (2005) *Phaeocystis* blooms in the global ocean and their controlling mechanisms: a review. *Journal of Sea Research*, **53**, 43–66.

Shelford EJ, Middelboe M, Moller EF, Suttle CA (2012) Virus-driven nitrogen cycling enhances phytoplankton growth. *Aquatic Microbial Ecology*, **66**, 41–46.

Staniewski MA, Short SM (2014) Potential viral stimulation of primary production observed during experimental determinations of phytoplankton mortality. *Aquatic Microbial Ecology*, **71**, 239–256.

Sunda WG, Cai WJ (2012) Eutrophication induced CO_2-acidification of subsurface coastal waters: interactive effects of temperature, salinity, and atmospheric PCO_2. *Environmental Science and Technology*, **46**, 10651–10659.

Suttle CA, Chan I, Cottrell MT (1991) Use of ultrafiltration to isolate viruses from seawater which are pathogens of marine phytoplankton. *Applied and Environmental Microbiology*, **57**, 721–726.

Suttle CA (1992) Inhibition of photosynthesis in phytoplankton by the submicron size fraction concentrated from seawater. *Marine Ecology Progress Series*, **87**, 105–112.

Suttle CA, Chen F (1992) Mechanisms and rates of decay of marine viruses in seawater. *Applied and Environmental Microbiology*, **58**, 3721–3729.

Suttle CA (2007) Marine viruses – major players in the global ecosystem. *Nature Review Microbiology*, **5**, 801–812.

Traving SJ, Clokie MR, Middelboe M (2013) Increased acidification has a profound effect on the interactions between the cyanobacterium *Synechococcus* sp. WH7803 and its viruses. *FEMS Microbiology Ecology*, **87**, 133–141.

Weinbauer MG, Rowe JM, Wilhelm SW (2010). Determining rates of virus production in aquatic systems by the virus reduction approach. In: *Manual of Aquatic Viral Ecology* (eds Wilhelm SW, Weinbauer MG, Suttle CA), pp. 1–8. ASLO, Waco.

Weinbauer MG, Bonilla-Findji O, Chan AM, Dolan JR, Short SM, Šimek K, Suttle CA (2011) *Synechococcus* growth in the ocean may depend on the lysis of heterotrophic bacteria. *Journal of Plankton Research*, **33**, 1465–1476.

Weitz JS, Wilhelm SW (2012). Ocean viruses and their effects on microbial communities and biogeochemical cycles. *F1000 Biology Reports*, **4**, 17.

Supporting Information

Additional Supporting Information may be found in the online version of this article:

Table S1. Parameters of the seawater carbonate system under the high and low-pH (HpH and LpH) levels in the *Phaeocystis globosa* cultures with or without the virus added. Dissolved inorganic carbon (DIC), pH, salinity, nutrient concentration, and temperature were used to derive all other parameters using a CO_2 system analyzing software (CO2SYS). Each datum represents the mean ± SD (n = 21).

Figure S1. Flow cytometry signature of the 0.2 μm-pore filtrate, after staining with SYBR Green, from PgV-infected *P. globosa* cultures. The green dots are from PgVs, and the other points are noise.

Figure S2. Effective photochemical quantum yield (a) and cell density (b) of *P. globosa* and abundance of PgV (c) during viral infection of ambient air grown cultures. Open symbols represent uninfected cultures, while the solid symbols represent cultures to which PgVs were added at the time indicated by the arrows. The data represent the mean ± SD (n = 3, triplicate cultures).

Figure S3. PCA analysis of rETR vs Irradiance for all treatments. The upper panel (scores plot) shows tight clustering of treatments indicating strong effects of virus infection and of CO_2 level (squares = LC − virus, circles = HC − virus, triangles = LC + virus, diamonds = HC + virus). The loadings plot (lower) indicates that the clustering in the scores was due mostly to values at higher irradiance.